ELSEVIER

Catalysis Today 48 (1999) 93–100

CATALYSIS TODAY

Liquid-phase methanol synthesis in apolar (squalane) and polar (tetraethylene glycol dimethylether) solvents

Gerard P. van der Laan, Antonie A.C.M. Beenackers*, Baiquan Ding[1], Johan C. Strikwerda

Department of Chemical Engineering, University of Groningen, Nijenborgh 4, 9747 AG, Groningen, Netherlands

Abstract

The kinetics of the three-phase methanol synthesis over a commercial Cu–Zn–Al_2O_3 catalyst were studied in an apolar solvent, squalane and a polar solvent, tetraethylene glycol dimethylether (TEGDME). Experimental conditions were varied as follows: P=3.0–5.3 MPa, T=488–533 K and $\Phi_{vG}/w=7.5\times10^{-3}$–$8\times10^{-3}$ Nm^3 s^{-1}kg$_{cat}^{-1}$. The nature of the slurry–liquid influences the activation energy and the kinetic rate constant by interaction between adsorbed species and solvent and by competitive adsorption of the solvent on the catalyst surface. The rate of reaction to methanol observed in TEGDME appeared to be about 10 times lower than in squalane. TEGDME reduces the reaction rate, which is a disadvantage for its use as a solvent.

Keywords: Methanol synthesis; Liquid-phase; Reaction kinetics; Solvent; Slurry-phase

1. Introduction

Methanol is an industrially important chemical which is produced at an annual rate of over 20 million tons worldwide. Methanol is widely used as a feedstock in various chemical applications and can also be used as a transportation fuel or a fuel additive. A considerable amount of methanol is used for the production of methyl *tert*-butyl ether (MTBE), a rapidly growing octane enhancer for the automotive market. Because of its favorable properties it may penetrate the transportation fuel market in a large scale. If so, the current scale with packed (multi-tube) beds of typical 1000 ton/day will be too small by 2 orders of magnitude. Therefore, new production technologies are needed, suitable for methanol production at the scale of 10^5 ton/day.

Conventionally, methanol is produced in two-phase gas–solid processes [1]. The solid phase is the catalyst and the gas phase consists of a mixture of reactants (CO, CO_2, and H_2) and products (CH_3OH and H_2O). The so-called low-pressure synthesis processes are operated in an adiabatic quenched reactor system (the ICI system) or in an internally cooled multitubular reactor (the Lurgi system). Both reactor types are operated at temperatures from 480 to 560 K at a pressure of about 5.0 MPa using Cu/Zn/Al catalysts. The methanol production rate is limited by the catalyst activity, the chemical equilibrium and the sensitivity of the catalyst to higher temperatures. The overall reactions important for the methanol synthesis are:

---

*Corresponding author. Tel.: +31-50-3634486; fax: +31-50-3634479; e-mail: a.a.c.m.beenackers@chem.rug.nl

[1] Present address: Department of Chemical Engineering, East China University of Science and Technology, 130 Meilong Road, Shanghai 200237, China.

0920-5861/99/$ – see front matter © 1999 Elsevier Science B.V. All rights reserved.
PII: S0920-5861(98)00362-9

Methanol synthesis reactions:

$$CO + 2H_2 \leftrightarrows CH_3OH \quad (1)$$

$$CO_2 + 3H_2 \leftrightarrows CH_3OH + H_2O \quad (2)$$

Reverse water–gas-shift reaction:

$$CO_2 + H_2 \leftrightarrows CO + H_2O \quad (3)$$

Recently, a three-phase methanol synthesis process was commercialized by Chem. Systems [2] under the trademark LPMEOH. Here, a gas–liquid slurry reactor is applied where the catalyst is kept in suspension by an inert liquid. One of the aims of the liquid is to provide a heat sink for the exothermal reaction. The inventors claim the following advantages in comparison with the conventional Lurgi or ICI systems: (i) superior temperature control because of excellent heat transfer characteristics; (ii) high conversion per pass; (iii) no diffusion limitations; (iv) low pressure drop over the reactor; (v) low gas recycle ratio; and (vi) stable reactor temperatures, resulting in longer catalyst life. An important advantage of a slurry system might be the possibility to scale-up the technology to capacities typical for transport fuel applications. A pilot plant based on the LPMEOH process with a capacity of 10 ton/day was described by Roberts et al. [3]. The slurry bubble column with an inner diameter of 0.67 m and liquid height of about 6 m was tested with low-pressure methanol-synthesis catalysts ($Cu/ZnO/Al_2O_3$) suspended in paraffinic or naphthenic oils. The concept of the solvent methanol process [4] is to introduce a high-boiling solvent in a suitable reactor (trickle bed or slurry bubble column) in co-current flow with the synthesis gas. The solvent selectively absorbs methanol as soon as it is formed, resulting in a low methanol activity at the catalyst surface thus leading to high single pass conversions. This way, the gas recycle can be reduced, or ideally eliminated. Flashing of the solvent delivers methanol and the lean solvent can be pressurized and recirculated to the reactor.

At present, several companies and universities are investigating the three-phase methanol synthesis process [1,5]. Up till now, the influence of the nature of the liquid on the intrinsic reaction rates has hardly been published. Roberts et al. [6] studied the effect of the slurry liquid on the activity and selectivity of a zinc chromite catalyst for the synthesis of methanol in a slurry reactor at temperatures between 598 and 648 K and a total pressure of 13.8 MPa. The kinetics were measured in three slurry liquids that were sufficiently stable at these temperatures and pressures: decahydronaphthalene (DHN, $C_{10}H_{18}$), tetrahydronaphthalene (THN, $C_{10}H_{12}$), and tetrahydroquinoline (THQ, $C_9H_{11}N$). The rate of methanol synthesis was high in THQ, while a low activity was obtained in THN. The latter solvent had a low selectivity to methanol and high hydrocarbon selectivity, relative to the other two liquids. No mechanistic explanation was given to describe the large differences in catalyst activity and selectivity to methanol. In this contribution we present data on the reaction rates of the methanol synthesis in two other solvents, an apolar solvent squalane and a polar solvent (tetraethylene glycol dimethylether, TEGDME; dipole moment ≈ 4 Debeije).

2. Experimental

2.1. Equipment

A well-mixed fed batch gas–slurry reactor was used. The experimental set-up is shown in Fig. 1. Experimental conditions were varied as follows: P=3.0–5.3 MPa, T=488–533 K, and $\Phi_{vG}/w=7.5\times10^{-3}$–$8\times10^{-3}$ $Nm^3\ s^{-1}\ kg^{-1}_{cat,ox.}$.

The individual syngas components were mixed in a separate feed gas compression system. The purities of the synthesis gas components were $H_2 \gg 99.999$ mol%, $CO \gg 99.8$ mol% and $CO_2 \gg 99.999$ mol%. The gas mixture was fed to a compressor which compressed the gas into a gas cylinder. The syngas was fed to the reactor through a mass flow controller and via two purification columns to remove catalyst poisons such as iron carbonyls, hydrogensulphide and oxygen, before entering the reactor. These columns were packed with BASF R3-11 and BASF R5-10 catalysts at 473 and 413 K, respectively.

The $0.35\times10^{-3}\ m^3$ stainless steel autoclave was connected to a magnetic stirrer. The shaft of the impeller in the reactor was hollow with small holes in the stirrer blades and sleeves in the top of the shaft. This enabled the vapor in the reactor to be recycled through the liquid by the suction created by the impeller. Above N=15 rev s^{-1} strong circulation of

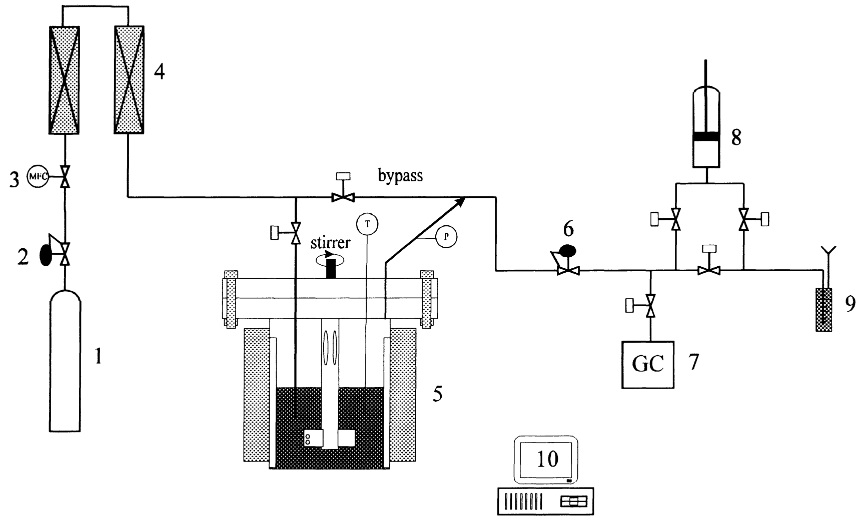

Fig. 1. Experimental set-up: (1) gas supply cylinder CO, CO_2, H_2; (2) pressure controller; (3) mass flow controller (MFC); (4) purification columns; (5) gas–slurry reactor; (6) back pressure reducer (BPR); (7) on-line GSC analysis; (8) flow meter; (9) bubble bottle; (10) personal computer; PI=pressure indicator; P=pressure measurement and controller; T=temperature measurement and controller.

the gas in the autoclave was observed. The impeller was always driven at N=33 rev s^{-1} to ensure complete mixing of the liquid and gas phase, a uniform distribution of the catalyst, and high mass and heat transfer rates. Vortex formation was prevented by four vertical baffles with a width of 8×10^{-3} m each. The reactor was electrically heated, and the temperature was measured with a PT-100 resistance thermometer (range: 273–773 K; accuracy: 0.2 K). The reactor pressure was measured (range: 0.1–10.0 MPa; accuracy: 0.01 MPa) and controlled by a pressure reducer in the reactor outlet, which was connected to a PID controller. A porous filter (5 μm), placed under the liquid level, was used for the gas distribution.

Downstream of the pressure reducer, a sample flow was split from the main flow and led to a heated injection valve of an on-line gas chromatograph (GC) [7]. To avoid condensation, the product gas lines were heated at 473 and 373 K upstream and downstream the needle valve, respectively. The product gas flow rate was measured via the displacement of a thermostated (373 K) mercury-sealed piston in a glass tube. Blank experiments showed that the packed purification columns and the reactor, without catalyst and half-filled with squalane, caused no significant conversion of syngas.

2.2. *Catalyst*

The catalyst applied was a mixture of CuO (55 wt%), ZnO (25 wt%), and Al_2O_3 (8 wt%)(commercial Haldor Topsøe MK 101). Properties of the catalyst were reported by Dybkjaer [8]. It was crushed and sieved to a particle size of 40–65 μm, in order to eliminate the influence of pore diffusion resistances [9].

2.3. *Liquid medium*

In order to study the effect of the nature of the solvents on kinetics, solvents were selected on the basis of varying specific properties such as apolarity (squalane), and polarity (tetraethylene glycol dimethylether=TEGDME). See Table 1 for the purity and source of the solvents used. TEGDME was identified as one of the potential solvents [10] for the solvent methanol process in view of its miscibility with methanol, a high normal boiling point (548 K), excellent thermal stability, and high solubility for the products relative to the reactants.

2.4. *Analysis*

A Hewlett-Packard 5980A gas chromatograph was used for on-line analysis of both the feed and the

Table 1
Purity and source of the solvents

Name	Formula	Source	Purity (mass %)
Tetraethylene glycol dimethylether (TEGDME)	$C_{10}H_{22}O_5$	Fluka AG	>99
Squalane	$C_{30}H_{62}$	Janssen Chimica	>99

product gas. It was equipped with a heated 10-port gas injection valve with two different sample loops of 0.07 and 1.95 cm^3 to determine the concentrations over a wide range, a capillary column (0.53 mm i.d., 25 m fused silica coated with a Poraplot Q film with thickness 0.020 mm) with helium or nitrogen as carrier gas with a linear velocity of 0.2 m s^{-1}, and a TCD (548 K; reference flow, 0.50 cm^3 s^{-1}) and FID (548 K; hydrogen flow, 0.53 cm^3 s^{-1}; air flow, 7.5 cm^3 s^{-1}) placed in series. The initial temperature of the column (303 K) was gradually increased according to an optimized temperature program. Chromatographic peak integration was performed by Hewlett-Packard 3396A and 3393A integrators for the TCD and FID, respectively.

Since the thermal conductivity of hydrogen almost equals that of the carrier gas helium, detection is very difficult due to negative peaks, non-linearity, and poor sensitivity. Therefore, hydrogen was determined in a separate analysis with nitrogen as the carrier gas.

The mole fractions of the components were calculated from the peak areas (A_i) correcting for fluctuations in the atmospheric pressure, according to

$$y_i = C_i A_i / P_{\mathrm{atm}}, \tag{4}$$

where C_i is the calibration factor for component i at 0.1 MPa. The calibration constants were periodically determined by calibration of the equipment with H_2, CO, CO_2, and CH_3OH standard mixtures of known composition. The TCD was calibrated for water by injection of a gas flow with a known concentration of water. The concentration of water in the carrier gas nitrogen was adjusted with two mass flow controllers and a continuous evaporator mixer from Bronkhorst (Ruurlo, Netherlands).

2.5. Experiments

Before the experiments were started, the catalyst was reduced according to an in situ activation procedure developed and patented by Air Products and Chemicals [11]. A mixture of 5 mol% H_2 in N_2 was fed to the reactor with a flow of 3.3×10^{-4} $Nm^3\ s^{-1}\ kg_{cat}^{-1}$ at 3.0 MPa. The reduction procedure followed a well-defined temperature program with temperature changes of 0.017 K s^{-1}. When the water fraction in the reactor outlet had become undetectable, indicating a complete reduction, syngas was supplied to the reactor. After four days, the catalyst had lost its "hyperactivity" and the composition of the product stream had become constant.

A standard experiment was repeated periodically to determine deactivation of the catalyst. To minimize the number of experiments and to get unbiased conclusions on the influence of the nature of the liquid on the kinetics, an experimental statistical design was adopted with both temperature and total pressure as variables for two different synthesis gas compositions. Table 2 shows the details of the experimental conditions of measurements with squalane and TEGDME.

Reaction rates for water and methanol were calculated from simple material balances over the reactor:

$$R_{\mathrm{CH_3OH}} = y_{\mathrm{CH_3OH}} \frac{\Phi_{\mathrm{v}}}{W} \frac{P_0}{RT_0}, \tag{5}$$

$$R_{\mathrm{H_2O}} = y_{\mathrm{H_2O}} \frac{\Phi_{\mathrm{v}}}{w} \frac{P_0}{RT_0}. \tag{6}$$

In these equations P_0 and T_0 correspond to normal conditions at 0.1 MPa and 293 K and y_i based on the concentration in the product gas from the reactor. Φ_{v} is the volumetric flow rate of the reactor effluent corrected to P_0 and T_0.

For each experiment the atomic balances of atomic species C, H, and O in the product and feed were checked. The deviations in these material balances were always very small, usually less than 1%.

3. Results and discussion

Reference experiments with standard gas showed no significant deactivation. A simplified model is used

Table 2
Experimental conditions for the kinetic gas–slurry experiments (slurry 1.5×10^{-3} kg crushed Cu/ZnO/Al_2O_3 catalyst (50–60 µm) suspended in 0.160 kg TEGDME (feed number 1–3) or squalane (feed number 4–5))

Feed number	Feed composition			P (MPa)	T (K)	$10^3\Phi_v/w_{cat}(Nm^3s^{-1}kg_{cat}^{-1})$
	y_{CO}	y_{CO_2}	y_{H_2}			
1[a]	0.125	0.051	0.824	3.0	503.2	7.7
2	0.081	0.101	0.828	3.0–5.3	487.4–532.7	7.6
3	0.219	0.048	0.733	3.0–5.3	487.4–533.1	7.6
4[a]	0.153	0.050	0.797	3.0	503.2	7.7
5	0.110	0.110	0.780	3.0–5.3	488.4–533.5	7.7

[a] Reference conditions for standard experiments.

to describe the reaction rate for methanol [9,12]. Though, the validity of the simplified model is restricted to a small range of conditions only, it is accurate enough to compare solvent effects on the rate of reaction:

$$R_{CH_3OH} = k\left(f_{H_2} - \frac{f_{CH_3OH}}{f_{CO}f_{H_2}K}\right). \tag{7}$$

The gas phase fugacities were calculated as follows:

$$f_i = y_i\varphi_{iG}P \tag{8}$$

with the gas phase fugacity coefficients φ_{iG} in Eq. (8) from the Soave–Redlich–Kwong equation of state [13,14].

For the temperature dependence of the equilibrium constant of the formation of methanol, K, the following relation was used [9] (pressures in bars):

$$\log K = \frac{5139}{T} - 12.621. \tag{9}$$

The relevant kinetic parameters, k and E_A, were calculated from the experimental data by minimizing the χ^2 function with the Levenberg–Marquardt method [15]:

$$\chi^2 = \sum_i \frac{(R_i^{exp} - R_i^{mod})^2}{\sigma_i^2}, \tag{10}$$

where R_i^{exp} is the experimental reaction rate of methanol, R_i^{mod} is the model prediction of the reaction rate and σ_i^2 is the variance of the experimental reaction rates. To speed up convergence, the kinetic constant was rewritten according to Froment [16]:

$$k(T) = k(T_m)\exp\{-E_A/R)(1/T - 1/T_m)\}, \tag{11}$$

where T_m was 510 K. The MARR (mean absolute relative residual) function, indicating the mean relative error, was applied to describe the accuracy of the fitted model on the experimental data:

$$\text{MARR} = \sum_j^N \left|\frac{R_j^{exp} - R_j^{mod}}{R_j^{exp}}\right| \frac{1}{N} \times 100\%. \tag{12}$$

See Table 3 for the MARR values and the optimized kinetic parameters for the methanol synthesis in TEGDME and squalane. Parity plots of the experimental and calculated reaction rates for methanol in TEGDME and squalane are presented in Fig. 2. This figure shows that the agreement between model and experiment is not impressive. This is caused by the adoption of a simplified model, that does not account for the formation of methanol via CO_2 and inhibition of adsorbed species. Remarkable is the great difference in activity between TEGDME and squalane. The kinetic rate constant at 510 K is about 10 times the

Table 3
Final estimate of the kinetic parameters in TEGDME and squalane and accuracy of the fitted model

Liquid	k (510 K) (mol s^{-1} kg^{-1} MPa^{-1})	E_a (kJ mol^{-1})	N	MARR (%)
TEGDME	0.248×10^{-3}	39.7	17	19.5
Squalane	2.05×10^{-3}	61.1	8	12.1

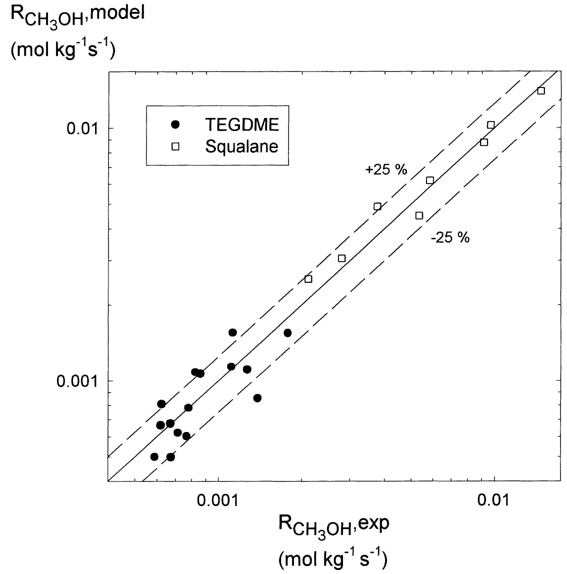

Fig. 2. Parity plot for the methanol reaction rates in TEGDME and squalane.

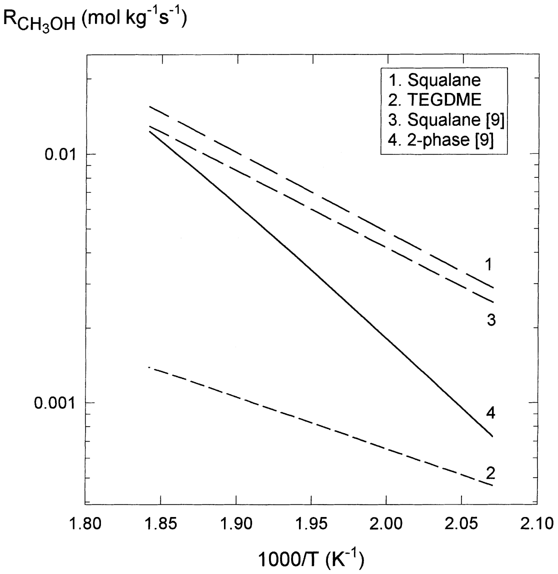

Fig. 3. Comparison of initial reaction rates for methanol in: squalane, TEGDME, squalane [9], and two-phase gas–solid system [9]. P=4.0 MPa; feed composition y_{CO}=0.15; $y_{CO_2}=0.05$; $y_{H_2}=0.80$.

value observed in TEGDME. Furthermore, TEGDME reduced the activation energy in comparison to squalane. This indicates that the polar solvent increases the rate of the rate determining step with a polar precursor [9]. For comparison, the results obtained from calculations based on reaction kinetics are plotted for the two-phase kinetics [9] and the three-phase kinetics in TEGDME and squalane in Fig. 3. The kinetic rate expressions for the reaction rate of methanol in squalane obtained by Graaf [9] are also included for comparison. It can be seen that the influence of the temperature differs between the two- and three-phase systems. For both solvents, the three-phase system is much less sensitive to the temperature. The rate of reaction observed in TEGDME is lower and in squalane is higher than in the two-phase system. The reaction rate in squalane measured by Graaf [9], shows the same behavior as our measurements. The kinetic experiments of Graaf [9] were carried out after 20 days time on stream, explaining a lower catalyst activity compared to our measurements.

From a literature review concerning the influence of a liquid-phase on the heterogeneous reaction kinetics in general, we conclude:

1. The rate of reaction is not significantly affected by introducing an *ideal* (non-adsorbing, inert, non-polar) liquid. So, the liquid does not affect the adsorbed surface species [17].
2. Competitive adsorption of a liquid on active catalytic sites will reduce the reaction rates [18–20].
3. The liquid can interact with weakly adsorbed surface species and can either increase or decrease the reaction rate in comparison with the vapor phase reaction [20,21].
4. Difference in solubility of reactants and products in various solvents explains the difference in liquid-phase concentration [4,17]. The reaction rate is enhanced, compared to the rate in the ideal liquid or the gas phase, if the solvent is similar to the reactants (high solubility) and vice versa [22].

The effect of the solvent on the rate of homogeneous chemical reactions has been correlated quantitatively with various physical properties (Lewis acidity, Lewis basicity, polarity, and polarizability) or with (semi)empirical parameters [23–25] describing interactions between the substrate and solvent. In heterogeneous systems, the number of interactions is increased due to the presence of the catalyst. In their review, Ĉervený and Růžička [20] reported data on the hydrogenation of cyclohexene on a 5% Pt on silica gel catalyst in 19 different solvents. They used the Drougard–Decroocq equation for describing the solvent effect on the rates of hydrogenation relative to standard reaction conditions:

$$\log(k_n/k_0) = \lambda\tau, \tag{13}$$

where τ characterizes the solvent and λ is the parameter of sensitivity of the reaction rate constant k_n relative to a reference solvent (k_0). Hydrogenation rates were correlated successfully with λ=1. The difference between the parameter τ for methanol (reference solvent) and other solvents is large for solvents containing a benzene ring. Ĉervený and Růžička [20] concluded that solvents affect complex interactions in three-phase systems, which can be related to solvent parameters for the same reaction conditions, catalysts, and reactants.

Stenger and Satterfield [17,26] measured the effect of the nature of an inert liquid on the rate of reaction and the selectivity of the Fischer–Tropsch synthesis. They observed the reaction rate in the Fischer–Tropsch synthesis in the presence of phenantrene nearly twice that in *n*-octacosane and triphenylmethane, even though the solubility is moderately less in phenantrene. The presence of phenantrene caused reduction of deposit formation (catalyst deactivation) and readsorption of primary products onto the catalyst and hence inhibited secondary reactions. Graaf et al. [21] observed a significant contribution of the methanol formation via CO_2 by introducing squalane in comparison with the two-phase system. The three-phase methanol synthesis in squalane is much less sensitive to the temperature. This suggests interaction between liquid and adsorbed species to be dominant over liquid adsorption. Breman et al. [27] measured the kinetics of the gas–slurry methanol-higher alcohol synthesis from $CO/CO_2/H_2$ in *n*-octacosane. The presence of *n*-octacosane as a slurry liquid affected the product distributions in comparison with the corresponding gas–solid system.

The solubilities of H_2 and CO were measured in both squalane and TEGDME [9,10]. Table 4 lists values at 498 K. Notably the solubilities of H_2 and CO are moderately lower in squalane relative to TEGDME. Despite this, the rate of reaction in squalane appears to be more than 10 times faster than in TEGDME. The latter solvent is much more polar than squalane and is supposed to adsorb more strongly onto the catalyst carrier.

Table 4
Equilibrium liquid phase concentrations of the reactants in TEGDME [10] and squalane [9] interpolated to 498 K in mol m^{-3} and y_{CO}=0.15 and y_{H_2} = 0.80 at P=3.0 MPa

Liquid	H_2 (mol m^{-3})	CO (mol m^{-3})
TEGDME	119.8	31.9
Squalane	94.8	22.0

4. Conclusions

From the above discussion, we conclude that (1) a slurry liquid (TEGDME or squalane) affects the activity of the catalyst via interaction between liquid and adsorbed surface species and (2) competitive adsorption of a polar solvent onto the catalyst carrier will reduce the reaction rate significantly. The observed activation energy appeared to decrease in the following order: two-phase>three-phase (squalane)>three-phase (TEGDME). This indicates that the polar solvent TEGDME stabilizes the rate of an elementary reaction step of a polar precursor in comparison to the two-phase process and squalane. On the other hand, the latter conclusion suggests TEGDME to reduce the reaction rate of methanol synthesis due to adsorption on the catalyst surface. TEGDME has excellent thermal stability and is the strongest solvent for the methanol components [4], but appears to reduce the intrinsic reaction rate in comparison to squalane according to this study.

5. Nomenclature

A	integrated area gas-phase component (counts)
C	calibration factor gas chromatograph (MPa counts^{-1})
E_A	activation energy (kJ mol^{-1})
f	partial fugacity (MPa)
k	pseudo reaction rate constant (mol s^{-1} kg^{-1} MPa^{-1})
K	chemical equilibrium constant (dimensionless)
MARR	mean absolute relative residual (dimensionless)
N	total number of experiments (dimensionless)

P	total pressure (MPa)
R	gas constant (J mol^{-1} K^{-1})
R_j	rate of reaction component j (mol $\mathrm{kg}_{\mathrm{cat}}^{-1}\,\mathrm{s}^{-1}$)
T	temperature (K)
w	weight of catalyst (kg)
x	mole fraction liquid phase (dimensionless)
y	mole fraction gas phase (dimensionless)

Greek symbols

χ	function for Levenberg–Marquardt optimization (dimensionless)
Φ_v	gas flow rate at standard conditions (T=293 K, P=1 bar) ($\mathrm{m}^3\ \mathrm{s}^{-1}$)
φ	fugacity coefficient (dimensionless)
λ	parameter of Eq. (13), sensitivity of reaction rate to a change in solvent
σ	function for Marquardt–Levenberg optimization (dimensionless)
τ	parameter of Eq. (13), effect of solvent on reaction rate (dimensionless)

Subscripts

act	activation
i	component: CO, CO_2, H_2, H_2O, CH_3OH
j	experiment number
G	gas phase
L	liquid phase
n	solvent
m	mean value
0	reference or standard conditions

Acknowledgements

The authors acknowledge fruitful discussions with J. Gmehling (Oldenburg), free delivery of MK-101 catalyst by Haldor Topsøe (Copenhagen) and the technical support of O.K.B. Staal, J.W. Bolhuis, and J.H. Marsman.

References

[1] J. Skrzypek, J. Sloczynski, S. Ledakowicz, Methanol Synthesis, Polish Scientific Publishers, Warszawa, 1994.

[2] M.B. Sherwin, D. Blum, Liquid-phase methanol, Final report of Chem. Systems, Electric Power Research Institute, Research Project 317-2, EPRI AF-1291, 1979.

[3] G.W. Roberts, D.M. Brown, T.H. Hsiung, J.J. Lewnard, Ind. Eng. Chem. Res. 32 (1993) 1610.

[4] J.M. Berty, C. Krishnan, J.R. Elliott Jr., , CHEMTECH 20 (1990) 624.

[5] A. Cybulski, Catal. Rev.-Sci. Eng. 36 (1994) 557.

[6] G.W. Roberts, M.A. Márquez, M.S. McCutchen, C.A. Haney, Prep. Papers Am. Chem. Soc., Div. Fuel Chem. 42 (1997) 710.

[7] J.H. Marsman, B.B. Breman, A.A.C.M. Beenackers, J. High Res. Chrom. 16 (1993) 141.

[8] I. Dybkjaer, Chem. Eco. Eng. Rev. 13 (1981) 149.

[9] G.H. Graaf, Ph.D. Thesis, University of Groningen, Groningen, Netherlands, 1988.

[10] P. Khosla, C. Krishnan, J.R. Elliott Jr., J.M. Berty, Chem. Eng. Comm. 102 (1991) 35.

[11] D.M. Brown, T.H. Hsiung, P. Rao, G.W. Roberts, US Patent 4 801 574, 1989.

[12] C. Krishnan, J.R. Elliott Jr., J.M. Berty, Ind. Eng. Chem. Res. 30 (1991) 1413.

[13] G. Soave, Chem. Eng. Sci. 27 (1972) 1197.

[14] R.C. Reid, J.M. Prausnitz, B.E. Poling, The Properties of Gases and Liquids, 4th ed., McGraw-Hill, New York, 1987.

[15] W.H. Press, B.P. Flannery, S.A. Teukolsky, W.T. Vetterling, Numerical Recipes in Pascal, Cambrigde University Press, New York, 1989.

[16] G.F. Froment, AIChE J. 21 (1975) 1041.

[17] H.G. Stenger, C.N. Satterfield, Ind. Eng. Chem. Proc. Des. Dev. 24 (1985) 407.

[18] C.N. Satterfield, P.F. Way, AIChE J. 18 (1972) 305.

[19] J.J. Kipling, Adsorption from Solutions of Non-electrolytes, Academic Press, New York, 1965.

[20] L. Ĉervený, V. Růžička, Adv. Catal. 30 (1981) 335.

[21] G.H. Graaf, J.G.M. Winkelman, E.J. Stamhuis, A.A.C.M. Beenackers, Chem. Eng. Sci. 43 (1988) 2169.

[22] C.A. Eckert, Ind. Eng. Chem. 59 (1967) 21.

[23] K.F. Wong, C.A. Eckert, Ind. Eng. Chem. 62 (1970) 16.

[24] I.A. Koppel, V.A. Palm, in: N.B. Chapman, J. Shorter (Eds.), Advances in linear free energy relationships Chap. 5, Plenum Press, New York, 1972.

[25] C.D. Johnson, The Hammett Equation, Cambridge University Press, Cambridge, 1973.

[26] H.G. Stenger, C.N. Satterfield, Ind. Eng. Chem. Proc. Des. Dev. 24 (1985) 411.

[27] B.B. Breman, A.A.C.M. Beenackers, H.A. Schuurman, E. Oesterholt, Catal. Today 24 (1995) 5.